OPTIMIZATION OF THE COLLIMATION SYSTEM FOR THE CSNS/RCS

N. Wang#, M. Y. Huang, S. Y. Xu, S. Wang, Institute of High Energy Physics, Beijing, China

Abstract

Beam loss induced activation of the accelerator components is one of the primary concerns in designing a high intensity machine. The uncontrolled beam loss is required to be less than 1 W/m for hands-on maintenance of the machine. A two stage collimation system is designed in the Rapid Cycling Synchrotron (RCS) of the China Spallation Neutron Source (CSNS) to localize the beam losses in a restricted area. The parameters of the collimator are optimized in order to obtain high collimation efficiency. The final design of the collimation system is presented. The reliability of the collimation system is estimated for different working points and with closed orbit errors.

INTRODUCTION

The accelerator complex of the CSNS consists of an 80 MeV linac and a 1.6 GeV RCS [1]. The RCS accelerates a beam pulse of 1.56×10^{13} protons from 80 MeV to 1.6 GeV with repetition rate of 25 Hz. Beam loss induced activation is one of the primary concerns during the accelerator design [2]. In order to control the beam losses around the ring to an acceptable level, two stage collimation systems are often used to localize the beam losses to restricted areas [3]. In CSNS, many works have been done to optimize the collimation system in the RCS [4, 5]. The material and shape of the collimators are carefully chosen to obtain high collimation efficiency and low activation around the ring other than the collimation section.

In this paper, the final design of the collimation system is first described. Then, the collimation efficiency and beam loss distribution around the ring are determined by multi-particle tracking. Finally, the sensitivity of the collimation efficiency to the transverse tune and closed orbit errors are investigated.

COLLIMATION SYSTEM DESIGN

The RCS lattice has a four fold structure with four straight sections dedicated to beam injection, transverse beam collimation, extraction, and RF systems. Each of the straight sections consists of one 11 meter and two 3.8 meter dispersion free drift spaces. The transverse collimation system locates in a separate straight section between injection and extraction section. Another straight section with large dispersion function in the arc in front of the transverse collimation is dedicated to momentum collimation system. In the first stage, the momentum collimation will not be used, but the space is preserved for further consideration. The physical aperture of the RCS is 540 πmm·mrad transverse acceptance with momentum acceptance of 1%. The main parameters of the RCS are given in Table 1.

#wangn@ihep.ac.cn

Table 1: The Main Parameters of the RCS

Parameters	Symbol, unit	Value
Inj./Ext. energy	E_{inj}/E_{ext}, GeV	0.08/1.6
Circumference	C, m	228
Beam population	N_p, $\times10^{13}$	1.56
Harmonic number	h	2
Repetition frequency	f_0, Hz	25
Betatron tune	ν_x/ν_y	4.86/4.78
Ring acceptance	ε, πmm·mrad	540

The transverse collimation system is composed of one primary collimator and four secondary collimators. The primary collimator consists of four 0.17 mm thick tungsten scrapers, which are set either horizontal or vertical. The scrapers can move independently to adjust to different beam conditions. Four secondary collimators setting downstream of the primary collimator serve as absorbers. Each of the secondary collimators consists of four movable copper blocks with thickness of 200 mm. The shape of the secondary collimator is chosen to have circle cross section with an aperture larger than 540 πmm·mrad to maximize the collimation efficiency. All collimator plates can be adjusted individually. The nominal acceptances of the primary and secondary collimators are set to 350 πmm·mrad and 400 πmm·mrad, respectively. The optimistic phase advance of the secondary collimators is expected to be 21° according to Jeanneret's theory. The layout of the collimation system with the twiss parameters is shown in Fig.1.

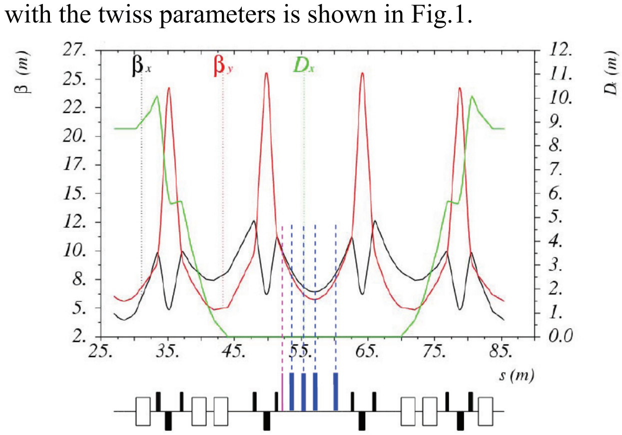

Figure 1: Lattice functions along a ring superperiod, and the layout of the collimation system (pink: primary collimator, blue: secondary collimators).

COLLIMATION EFFICIENCY

Using the collimation system described above, the collimation efficiency is estimated with the ORBIT code [7]. In the code, when a particle hits the collimator, ionization energy loss, multiple Coulomb scattering, nuclear elastic and inelastic interactions are considered. The collimation efficiency is defined as the ratio between the particles lost in the collimators and the total number of particles lost in the whole ring.

In order to estimate the collimation efficiency of the collimation system, a realistic beam distribution obtained by multi-turn painting injection, as shown in Fig. 2, is used. The 99% emittance of the beam distribution is about 290 πmm·mrad. Here, the uncorrelated painting has been used.

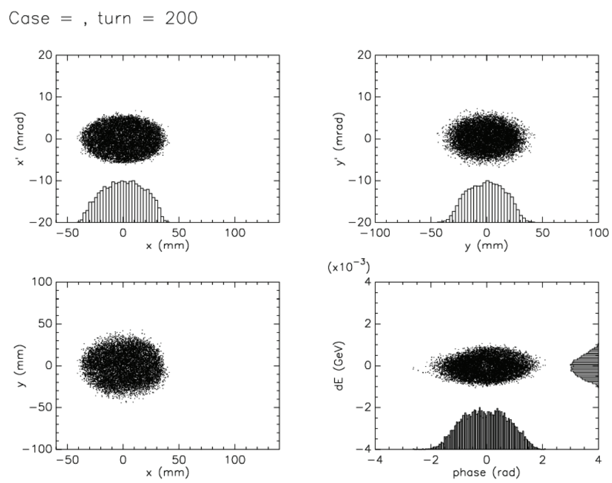

Figure 2: Phase space distribution of the beam for tracking simulation.

The beam is tracked and accelerated from 80 MeV to 1.6 GeV in the presence of space charge. The collimation efficiency and integrated beam loss versus time are shown in Fig. 3. The curves are obtained by tracking 10^6 macro-particles for about 5000 turns.

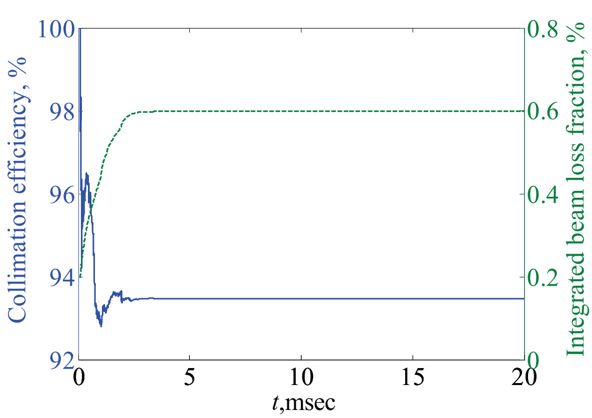

Figure 3: Collimation efficiency and integrated beam loss versus time.

The collimation efficiency varies with time, which indicates that the performance of the collimation system depends on the property of the beam lost. The resulting collimation efficiency is about 93% with total beam loss of 6×10^{-3}. The beam losses mostly occur in the first three mili-seconds when the space charge is strong. After that, the transverse beam emittance is shrinked with the energy increasing.

BEAM LOSS DISTRIBUTION

The beam loss distribution around the RCS is also investigated using the ORBIT code. The predicted beam loss in the accelerator components along the RCS is shown in Fig. 4. It is found that, the uncontrolled beam losses at the RCS components are less than 0.6 W/m. Over 96% of the beam loss is located within the collimation straight section.

Most of the uncontrolled beam losses locate downstream of the collimation system which are survived after nuclear scattering with the collimators. Another part of the uncontrolled beam losses concentrated at the injection region is induced by the scattering of the injection foil. Some losses in the arc section are due to the RF trapping inefficient during the beam acceleration.

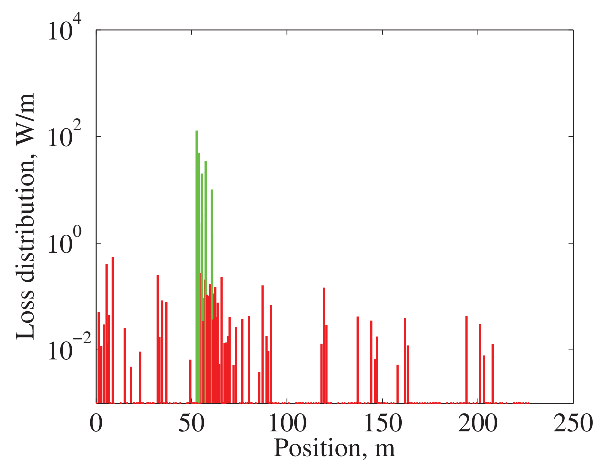

Figure 4: Predicted beam loss distribution around the RCS. The green lines represent losses to the collimators, and the red lines represent losses to ring apertures.

RELIABILITY OF THE COLLIMATION SYSTEM

The performance of the collimation system depends on the design parameters of the RCS. In addition, the collimation system design needs to be flexible to accommodate different beam conditions without compromising the collimation efficiency. The sensitivity of the collimation efficiency to the transverse tune and closed orbit errors are investigated.

Tune Dependence

The performance of the collimation system is investigated for two transverse tunes other than the nominal tune. For both cases, the apertures of the collimators are adjusted according to the lattice to keep high collimation efficiency. The acceptance of primary

ISBN 978-3-95450-115-1

collimator is fixed to 350 πmm·mrad, and the acceptance of all secondary collimators is set to 400 πmm·mrad in the simulations. The collimation efficiency and uncontrolled beam losses are compared with the results obtained in the nominal case as given in Table 2. The collimation system is still efficient under different working points. In both cases, beam losses are well localized in the collimation section.

Table 2: Simulation Results for Different Transverse Tunes

Transverse tune (νx/νy)	Collimation efficiency	Uncontrolled beam loss
4.86/4.78	93.5%	5.2E–4
4.82/4.36	95.6%	7.7 E–3
5.82/4.80	91.1%	8.1E–3

Closed Orbit Errors

The closed orbit distortion will affect the beam longitudinal dynamics and substantially change the physical aperture. Additional beam loss may occur with closed orbit errors. The closed orbit distortion due to dipole magnetic error is taken into account. A set of random dipole magnetic errors are added to the bending magnets. The resulting maximum closed orbit distortion in the RCS is from 1mm to 26 mm. The apertures of the collimators are adjusted according to the localized closed orbit deviation in the collimation section. The collimation efficiency and beam loss distribution around the ring are investigated. Fig. 5 shows the collimation efficiency and uncontrolled beam loss for different orbit errors.

From the result, a 5 mm closed orbit error causes an efficiency decrease of less than 1%. The estimated efficiency of the collimation system becomes 3% worse with a maximum closed orbit deviation of 15 mm. The collimation efficiency dramatically decreases with a closed orbit error larger than 20 mm, when the primary collimator is no longer the smallest aperture in the ring. The uncontrolled beam loss is still less than 1E–3 if the orbit error is smaller than 4 mm.

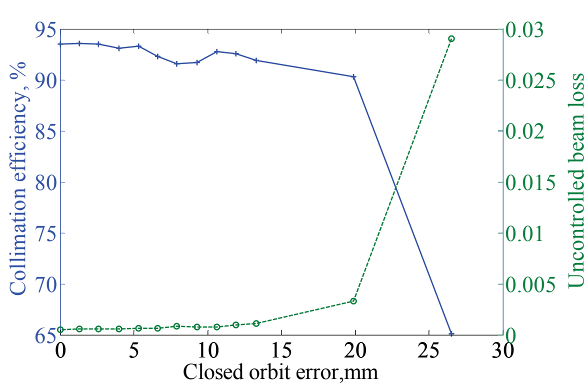

Figure 5: Collimation efficiency and integrated beam loss for different closed orbit errors.

CONCLUSIONS

A two stage collimation system has been designed and optimized for the RCS in CSNS. The system consists of one primary collimator and four secondary collimators. The collimation efficiency is estimated and shown to be larger than 90%. The beam loss distribution around the RCS is investigated. The beam losses are well localized in the collimation section and the uncontrolled beam loss outside the collimation region are well below 1 W/m. The uncontrolled beam losses of 5.2E–4 of the total beam is achieved.

The performance of the collimation system in the RCS is investigated for different betatron tunes. The collimation efficiency is larger than 90% in all the cases. Furthermore, the efficiency dependence on the closed orbit error is investigated. A maximum closed orbit error smaller than 5 mm in the ring causes a small decrease of collimation efficiency.

ACKNOWLEDGMENT

The authors would like to thank all the AP group and mechanical group members in CSNS project for their discussions and suggestions.

REFERENCES

[1] J. Wei et al., China Spallation Neutron Source Accelerator Design and R&D, Proc. of EPAC2006, Edinburgh, Scotland, p.366 (2006).
[2] J. Wei, Beam Cleaning in High-Power Proton Accelerators, in Proc. of ICFA Workshop on Beam Halo Dynamics, Diagnostics, and Collimation (HALO'03), Montauk, AIP Conf. Proc., vol. 693 (2003) pp.38-43.
[3] J. B. Jeanneret, Optics of a two-stage collimation system, PRST-AB vol. 1, 081001 (1998).
[4] T. Wei, Q. Qin, Nucl. Instr. Meth. Phys. Res. A 566 (2006) pp.212-217.
[5] N. Wang, S. Wang, N. Huang, and Q. Qin, The design of beam collimation system for CSNS/RCS, Proc. of HB2010, Morschach, Switzerland, pp. 572-575 (2010).
[6] S. Wang et al., The optimization of beam dynamics design for CSNS/RCS, Proc. of IPAC'10, Kyoto, Japan, p. 630 (2010).
[7] J. Galambos et al., ORBIT User's Manual, SNS/ORNL/AP Technical Note 011 (1999).